



Stochastic melonic kinetics with random initial conditions

Bio Wahabou Kpera^a, Vincent Lahoche^b, Dine Ousmane Samary^{a,b,*}

^a *International Chair in Mathematical Physics and Applications (ICMPA-UNESCO Chair), University of Abomey-Calavi, 072B.P.50, Cotonou, Republic of Benin*

^b *Université Paris Saclay, CEA List, Gif-sur-Yvette, F-91191, France*

Received 17 February 2023; received in revised form 29 March 2023; accepted 4 April 2023

Available online 6 April 2023

Editor: Stephan Stieberger

Abstract

The probability laws associated with random tensors or tensor field theories are traditionally equilibrium distributions. In this paper, we consider a stochastic point of view, and approach the quantization by a Langevin type equation. We especially address the low-temperature behavior of the phase ordering kinetics of a stochastic complex tensor field $T_{i_1 \dots i_d}(x, t)$ of size N and rank d in dimension D . The method we propose use the self averaging property of the tensorial invariants in the large N limit. In this regime, the dynamics is governed by the melonic sector, whose behavior is studied in the quenched limit, where the contractions involving $d - 1$ indices self-average around a diagonal matrix proportional to the identity. The following work especially focuses on the cyclic (i.e. non-branching) melonic sector, and we study the way that the system returns to the equilibrium regime regarding the temperature and the shape of the potential. In particular, we provide a general formula for the transition temperature between these regimes. The manuscript is accompanied by numerical simulations to support the theoretical analysis, and essentially aims to open towards this new field of investigation.

© 2023 The Authors. Published by Elsevier B.V. This is an open access article under the CC BY license (<http://creativecommons.org/licenses/by/4.0/>). Funded by SCOAP³.

* Corresponding author.

E-mail addresses: wahaboukpera@gmail.com (B.W. Kpera), vincent.lahoche@cea.fr (V. Lahoche), dine.ousmanesamary@cipma.uac.bj (D. Ousmane Samary).

Contents

1. Introduction	2
2. Model and conventions	3
3. The $D = 0$ model in the quenched limit for a blank noise	6
3.1. Static limit	6
3.2. Equilibrium dynamics	7
3.3. Low temperature regime	10
3.4. Numerical study	13
4. Blank noise limit for $D > 0$: UV regularized theory below critical temperature	16
4.1. The quartic case	17
4.2. Time evolution and low-temperature expansion	20
4.3. Continuum limit	22
4.4. Higher order potentials	23
5. Disordered Langevin dynamics	27
6. Discussions and conclusion	30
CRediT authorship contribution statement	30
Declaration of competing interest	30
Data availability	30
References	30

1. Introduction

Phase ordering kinetics is a phenomenon classically describing the growth of an ordered phase as a domain coarsening for a quenched system, from the homogeneous phase toward a broken phase [1]. It has been investigated for $O(N)$ field theory models [2,4] from the methods used to solve spin glass dynamics, and physics exhibits exciting relation with the soft $p = 2$ spin dynamics [6–8,5,9,10]. In this paper, we investigate the growth of the leading order phase for a stochastic random tensor model (RTM), which in contrast with ordinary phase ordering kinetics does not break the underlying $U(N)^{\times d}$ symmetry.

RTMs were introduced to generalize in higher dimensions the success of random matrix models (RMM) for 2D quantum Einstein gravity [11]. In 2009, it is shown that the colored RTM admits a tractable $1/N$ expansion involving a generalized degree $\varpi \geq 0$ such that the Feynman amplitudes $A(\mathcal{G})$ for the graph \mathcal{G} scales as $A(\mathcal{G}) \sim N^{d - \frac{2}{(d-1)!} \varpi(\mathcal{G})}$ [12]. The degree ϖ can be computed from the set of vertices, edges, and faces building the graph \mathcal{G} , which is a 2-simplex rather than an ordinary Feynman graph. The leading order graphs called melons are defined by the condition $\varpi(\mathcal{G}) = 0$, and follow a recursive definition reminiscent of branched polymers occurring for large N random vectors [14]. Furthermore, their critical behavior has been investigated as well analytically [15,17], and confirms the branched polymer phase transition from the critical exponent. Recently the so called Sachdev–Ye–Kitaev (SYK) quantum mechanics model which consists of N -Majorana fermions with random interactions are showed to admit this same large N -limit [28–30]. Many other works in this direction have also been successful, in particular: the $O(N)$ -tensor model to derive the fate of the wormholes in a model without quenched disorder with gauge symmetry whose correlation function and thermodynamics in the large N limit are the same as that of the SYK model [31,32], see also [33–37] for similar works. Generally, what makes the RTM power countable is their global $U(N)$ invariance, and the statistics

of RTM follow an exponential law $\rho \sim e^{-S}$, where the classical action S is a sum of $U(N)^{\times d}$ invariants.

In this paper, we give an introduction to the new field of investigation i.e. the stochastic complex tensors $T_{i_1 \dots i_d}(x, t)$ on \mathbb{R}^{D+1} , whose dynamics follow a diffusion Langevin type equation, by focusing on the melonic cyclic (i.e. non-branched) sector. Such a stochastic model has been considered recently for a tensorial group field theory (TGFT) [18] where a gravitational field was expected to be out of equilibrium with respect to a weakly coupled scalar field playing the role of a physical ‘‘clock’’ and materialized by the time variable [16]. Our purpose in this manuscript is only to focus on the large time dynamics, where the random tensor is ‘‘quenched’’ around a mean value. In that limit, the closed equations can be solved with elementary analytic methods, and a transition temperature between a power law versus an exponential relaxation can be computed. However, these conclusions depend on the shape of the confining potential, and in particular on the order of the roots of the polynomial, which we also highlight. This kind of model is studied in the framework of vectors field theory in the large N -limit [2,3,6]. The generalization to the tensor case with a more complicated invariance for a multilinear object is therefore necessary.

Outline. The paper is organized as follows. In section 2 we define the model and conventions. In section 3 we consider the low-temperature regime for $D = 0$ in the quenched limit, and in section 4 we extend the method for $D > 0$. In both cases, we investigate the large time closed equation expected from the self-averaging assumption and the transition regime toward this limit. In section 5 the case of a disordered tensor for $D = 0$, the disorder coupling is materialized by the tensor product of Wigner matrices. We conclude in section 6.

2. Model and conventions

We consider a time-dependent complex tensor $\mathbf{T}(x, t)$ with rank $d > 2$, $t \in \mathbb{R}$ and $x \in \mathbb{R}^D$. We denote by $T_{i_1 \dots i_d}(x, t) \in \mathbb{C}$ the components of the tensor, and the indices i_1, \dots, i_d run from 1 to N . We furthermore denote by $\bar{\mathbf{T}}(x, t)$ the complex-conjugate tensor of $\mathbf{T}(x, t)$, and by $\bar{T}_{i_1 \dots i_d}(x, t)$ its components. The dynamics of the tensor are assumed to follow a Langevin-like equation:

$$\dot{T}_{i_1 \dots i_d} := -\frac{\delta \mathcal{H}}{\delta \bar{T}_{i_1 \dots i_d}} + \partial_x^2 T_{i_1 \dots i_d} + \eta_{i_1 \dots i_d}. \tag{1}$$

In this equation $\dot{T}_{i_1 \dots i_d}$ is the derivative with respect to t , ∂_x^2 denotes the standard Laplacian over \mathbb{R}^D , $\eta_{i_1 \dots i_d}(x, t)$ is a Gaussian tensor field with correlations defined as

$$\langle \eta_{i_1 \dots i_d}(x, t) \bar{\eta}_{j_1 \dots j_d}(x', t') \rangle = \prod_{c=1}^d \frac{\delta_{i_c j_c} e^{-\frac{|x-x'|^2}{2\Lambda^{-2}}}}{\Lambda^{-D} (2\pi)^{D/2}} F(t-t'), \tag{2}$$

where $F(t-t') = F(t' - t)$ is the memory function, and in the *blank noise limit*:

$$F(t-t') =: T \delta(t-t'), \tag{3}$$

the friction coefficient T being interpreted as the temperature for the equilibrium distribution, see below. The UV cut-off Λ provides a UV regularization of the theory, which will be clear in the next sections. Note that,

$$\lim_{\Lambda \rightarrow \infty} \frac{e^{-\frac{|x-x'|^2}{2\Lambda^{-2}}}}{\Lambda^{-D} (2\pi)^{D/2}} \rightarrow \delta(x-x'). \tag{4}$$

The Hamiltonian $\mathcal{H} \equiv \mathcal{H}[\mathbf{T}, \bar{\mathbf{T}}]$ is assumed to be a sum of tensorial invariant, namely:

$$\begin{aligned}
 \mathcal{H}[\mathbf{T}, \bar{\mathbf{T}}] = & \mu \text{ (bubble with 2 vertices)} + g_{21} \text{ (bubble with 4 vertices)} + \dots + g_{31} \text{ (bubble with 6 vertices)} + \dots \\
 & + g_{41} \text{ (bubble with 8 vertices)} + \dots,
 \end{aligned}
 \tag{5}$$

where we use standard convention in the RTM literature: black and white vertices materialize respectively fields \mathbf{T} and $\bar{\mathbf{T}}$, and solid edges materialize Kronecker Dirac delta between indices of different tensors. Furthermore, all the tensor fields are taken at the same point x and at the same time t for each interaction and the Hamiltonian involves a global integral over \mathbb{R}^D .

We call a *bubble* such a connected graph and note that we set $d = 3$ for graphical representations of bubbles in this paper. Note that high valence interactions avoid arbitrary large configurations for the stochastic tensor T . For a fixed initial condition for $t = t_0$, one can consider the probability $P[\mathbf{T}, \bar{\mathbf{T}}, t]$ that tensor takes the values $(\mathbf{T}(t) = \mathbf{T}, \bar{\mathbf{T}}(t) = \bar{\mathbf{T}})$ for time $t > t_0$. This probability satisfies a Fokker-Planck equation [20], and for a delta-correlated noise in space dimension zero, the equilibrium probability $\rho[\mathbf{T}, \bar{\mathbf{T}}] := \lim_{t \rightarrow \infty} P[\mathbf{T}, \bar{\mathbf{T}}, t]$ behaves as,

$$\rho[\mathbf{T}, \bar{\mathbf{T}}] \propto \exp\left(-2 \frac{\mathcal{H}[\mathbf{T}, \bar{\mathbf{T}}]}{T}\right),
 \tag{6}$$

which corresponds to a standard RTM at temperature T if the N -scaling of couplings constants μ and g_{ij} labeling each bubble are such that Feynman amplitudes $A(\mathcal{G})$ scale as $N^{d - \frac{2}{(d-1)} \varpi(\mathcal{G})}$. This can be achieved if coupling constants g_b for bubble b scales as $g_{ij} = N^{a(b)} \bar{g}_{ij}$ with:

$$a(b) := -(p - 1)(d - 1) - \frac{2}{(d - 2)!} \varpi(b),
 \tag{7}$$

where the valence $p := n(b)$ is the number of black vertices in b . Note that for melonic bubbles $\varpi(b) \equiv 0$.

In the next sections we investigate the large-time behavior in the $N \rightarrow \infty$ regime. In particular, we compute the transition temperature investigating, in the quenched regime, the effective dynamics for the self-averaging quantity:

$$r(x, t) \equiv \sum_{i_1 \dots i_d} \frac{\bar{T}_{i_1 \dots i_d}(x, t) T_{i_1 \dots i_d}(x, t)}{N^d}.
 \tag{8}$$

For our purpose in this paper, we focus on the cyclic sector of the melonic family, and we recall some definitions for self-consistency.

Definition 1. Any melonic bubble b_p of valence p may be deduced from the elementary melon b_1 :

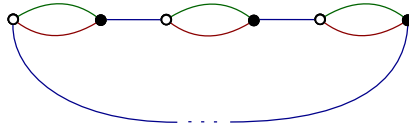


Fig. 1. Structure of the non-branching melons for $d = 3$.

$$b_1 := \text{diagram of a melon with two vertices and two edges (red and green)}, \tag{9}$$

replacing successively $(\kappa - 1)$ -colored edges (including maybe color “0”) by $(d - 1)$ -dipole, the $(d - 1)$ -dipole insertion operator \mathfrak{R}_c being defined as:

$$i \xrightarrow[c]{} c \text{---} \text{diagram of a melon} \tag{10}$$

or formula: $b_p := \left(\prod_{\alpha=1}^{p-1} \mathfrak{R}_{c_\alpha}\right) b_1$. This recursive definition solves the constraint $\varpi(b) \equiv 0$.

The cyclic melons are then defined as follows:

Definition 2. A non-branching melonic bubble of valence p , $b_p^{(\ell)}$ is labeled with a single color index $c \in \llbracket 1, d \rrbracket$, and defined such that:

$$b_p^{(c)} := (\mathfrak{R}_c)^{p-1} b_1. \tag{11}$$

Fig. 1 provides the generic structure of melonic non-branching bubbles in rank $d = 3$. We then assume that the Hamiltonian \mathcal{H} reads as

$$\mathcal{H}[T, \bar{T}] = \mu \text{diagram of a melon} + \sum_{c=1}^d \mathcal{V}_c[T, \bar{T}], \tag{12}$$

where $\mathcal{V}_c[T, \bar{T}]$ expands as:

$$\begin{aligned} \mathcal{V}_c[T, \bar{T}] &= N^{d-1} \sum_{p \geq 2} \frac{\bar{g}_p}{p N^{p(d-1)}} \text{diagram of a bubble with } p \text{ melons} \\ &=: N^{d-1} \sum_{p \geq 1} \frac{\bar{g}_p}{p N^{p(d-1)}} \text{Tr}(\Phi_c)^p, \end{aligned} \tag{13}$$

where entries of the unitary matrices Φ_c are defined as:

$$(\Phi_c)_{ij} := \sum_{I, J} \bar{T}_I T_J \left(\prod_{\ell \neq c} \delta_{i_\ell j_\ell} \right) \delta_{i_c j_c}, \tag{14}$$

such that $N^d r \equiv \text{Tr}(\Phi_c)$.

3. The $D = 0$ model in the quenched limit for a blank noise

This section is devoted to the dynamic aspects of the zero-dimensional model. Equation (1) can be investigated for a large time, and with some approximations that we will detail, the radius $r(t)$ satisfies a closed equation that can be studied analytically [2]. The way that the system converges toward equilibrium for late time can be investigated as well. The zero-dimensional model has no particular interest in itself, and the aim of this section is essential to introduce the general strategy that we will implement in the next two sections.

3.1. Static limit

The equilibrium points of our model are given by the relation:

$$0 = \frac{\partial \mathcal{H}}{\partial \bar{T}_{i_1 \dots i_d}} = \mu \left[\text{diagram} \right] + \sum_{c=1}^d \left(g_2 \left[\text{diagram} \right] + g_3 \left[\text{diagram} \right] + \dots \right), \tag{15}$$

where the deleted nodes correspond to the partial derivatives with respect to the field Φ_c . The vacuum solution can be chosen to be $U(N)$ invariant, namely¹:

$$(\Phi_c)_{ij}(t) = \kappa_c(t) \delta_{ij}, \tag{16}$$

which can be easily justified in the large N limit due to our random initial condition (22). We furthermore assume that color permutation symmetry is unbroken, and $\kappa_c \equiv \kappa, \forall c$. In that way, equation (15) becomes:

$$0 \equiv T_I \times \frac{\partial}{\partial \kappa} \left(\mu \kappa + d \sum_{p \geq 2} \frac{g_p}{p} \kappa^p \right) =: T_I \times \frac{\partial U(\kappa)}{\partial \kappa}, \tag{17}$$

where $I := i_1 \dots i_d$. Hence, assuming $T_I \neq 0$, the equilibrium points are defined by the minima of the potential $U(\kappa)$. For the quartic model, this point is given by:

$$\kappa = -N^{d-1} \left(\frac{\mu}{\bar{g}_2 d} \right) = \mathcal{O}(N^{d-1}). \tag{18}$$

If we assume that the system does not break the $U(N)$ symmetry dynamically and for large N Φ_c self average around a diagonal colored symmetric matrix during the time evolution (see Remark 1 at the end of this section), the Langevin equation (1) can be approached as:

$$\dot{T}_{i_1 \dots i_d} = -T_{i_1 \dots i_d} U'(\kappa) + \eta_{i_1 \dots i_d}, \tag{19}$$

where κ is assumed to be replaced by its averaged value, such that each component of T decouples from the others. The previous equation can be formally solved as:

$$T_{i_1 \dots i_d}(t) = T_{i_1 \dots i_d}(0) \rho(t) + \int_0^t dt' \eta_{i_1 \dots i_d}(t') \frac{\rho(t)}{\rho(t')}, \tag{20}$$

¹ A corollary of the standard Schur Lemma.

with:

$$\rho(t) := e^{-g(t)}, \quad g(t) := \int_0^t dt' U'(\kappa(t')). \tag{21}$$

In equation (20), the time $t = 0$ has to be understood not as a true initial condition but as an arbitrary time, far from the true origin of time. Because we have no information about the true behavior of the tensor at $t = 0$ for a given draw, we impose it to be randomly distributed accordingly with the centered Gaussian distribution²:

$$\langle \bar{T}_{i_1 \dots i_d}(x, 0) T_{j_1 \dots j_d}(x', 0) \rangle_0 = \Delta \prod_{c=1}^d \delta_{i_c j_c} \frac{e^{-\frac{|x-x'|^2}{2\Lambda^{-2}}}}{\Lambda^{-D}(2\pi)^{D/2}}, \tag{22}$$

where $|x|$ is the standard Euclidean norm, $\langle X \rangle_0$ means averaging over initial conditions and Λ is the same UV cutoff as for the noise $\eta(x, t)$. Hence we get the closed equation:

$$\boxed{r(t)G(t) = \Delta + T \int_0^t dt' G(t')}, \tag{23}$$

where $G(t) := e^{2g(t)}$. For large time, we expect that $r(t)$ reaches one of the equilibrium points of $U(\kappa)$, i.e., that $U'(\kappa(t)) \rightarrow 0$ for t large enough (see Section 4). From this expectation, the previous equation looks like a closed integral equation for $G(t)$, which can be easily solved asymptotically.

- For $T = 0$, we assume $r(t) \rightarrow r_0 \neq 0$ for t large enough, such that $U'(N^{d-1}r_0) = 0$. Hence, $G(t) \rightarrow \Delta/r_0$, and $U'(\kappa(t)) \rightarrow 0$, in agreement with our assumption. For $r_0 = 0$, if $\Delta \neq 0$, then $G(t)$ has to diverge with t , and $\langle T_{i_1, \dots, i_d} \rangle \rightarrow 0$.
- For $T \neq 0$, differentiating the closed equation concerning t , we get $\dot{G} \sim (T/r_0)G(t) \rightarrow G(t) \sim e^{(T/r_0)t}$, therefore $U'(\kappa(t)) \rightarrow (T/2r_0)$, and the system is repelled from the equilibrium point due to thermal fluctuations.

3.2. Equilibrium dynamics

The time evolution toward the asymptotic regime can be investigated with a little improvement of the previous argument. Indeed, assuming the validity of the quenching regime, and because from the definition:

$$U'(\kappa(t)) = \frac{1}{2} \frac{\dot{G}}{G}, \tag{24}$$

we have for the quartic model:

$$\frac{1}{2} \dot{G} = \mu G(t) + d\bar{g}_2 \left(\Delta + T \int_0^t dt' G(t') \right). \tag{25}$$

² We define arbitrary D here, despite this section focusing on the case $D = 0$.

Deriving the equation with respect to t , we have:

$$\ddot{G}(t) - 2\mu\dot{G}(t) - 2d\bar{g}_2TG(t) = 0. \tag{26}$$

This is a linear homogeneous differential equation of second order, that can be easily solved as a combination of exponential:

$$G(t) = \alpha e^{i\omega_+t} + \beta e^{i\omega_-t}, \tag{27}$$

where ω_{\pm} is the solution of the characteristic polynomial, namely:

$$\omega^2 + 2i\mu\omega + 2d\bar{g}_2T = 0, \tag{28}$$

explicitly:

$$\omega_{\pm} = -i\mu \left(1 \pm \sqrt{1 + \frac{2d\bar{g}_2T}{\mu^2}} \right). \tag{29}$$

We have two initial conditions. First $G(0) = 1$ leading to $\alpha + \beta = 1$. Secondly $\dot{G}(0) = 2U'(\kappa(0))$, i.e.

$$\dot{G}(0) = 2(\mu + d\bar{g}_2\Delta) = -2\mu \left(\frac{\Delta}{r_0} - 1 \right) \tag{30}$$

(see Remark 1 below) and where $r_0 := -\mu/(\bar{g}_2d)$. Hence, we must have:

$$i\omega_+\alpha + i\omega_-(1 - \alpha) = -2\mu \left(\frac{\Delta}{r_0} - 1 \right), \tag{31}$$

in other words,

$$\alpha = -\frac{2 \left(\frac{\Delta}{r_0} - 1 \right) + \left(1 - \sqrt{1 + \frac{2d\bar{g}_2T}{\mu^2}} \right)}{2\sqrt{1 + \frac{2d\bar{g}_2T}{\mu^2}}}, \tag{32}$$

and especially for $T = 0$:

$$\alpha = 1 - \frac{\Delta}{r_0}, \quad \beta = \frac{\Delta}{r_0}. \tag{33}$$

For $T = 0$, we find an exponential law $G(t) = \alpha e^{2\mu t} + \beta$ and the behavior of the system depends on the sign of μ . For $\mu < 0$, $G(t) \rightarrow \Delta/r_0$ exponentially, as expected. For $\mu > 0$, $U'(\kappa(t)) \rightarrow \mu$ for large time, and then $\kappa(t) \rightarrow 0$. Note that because $G(t)$ is positive, we must have $\Delta < r_0$ if we expect that the solution holds for all times. If $\Delta > r_0$, $G(t)$ vanishes for $t = \tau$,

$$\tau = \frac{1}{2\mu} \ln \left(\frac{1}{1 - r_0/\Delta} \right). \tag{34}$$

For $T \neq 0$, the two solutions ω_- and ω_+ have different signs, and in particular $i\omega_- < 0$. For small T :

$$\omega_- = -i\frac{T}{r_0} + \mathcal{O}(T^2), \tag{35}$$

and:

$$G(t) \sim \alpha e^{2\mu t} + \beta e^{(T/r_0)t}. \tag{36}$$

Hence for $\mu < 0$, we recover the asymptotic behavior expected from the previous analysis. As discussed previously for $T \neq 0$, the system fails to reach the equilibrium point of the potential. Nevertheless, it reaches an equilibrium regime that we can characterize. Indeed, from (27), we have for large time:

$$G(t) \sim \min_{i\omega_{\pm}} e^{i\omega_{\pm}t}, \tag{37}$$

or:

$$2U'(\kappa(t)) \sim \min_{i\omega_{\pm}} \mu \left(1 \pm \sqrt{1 + \frac{2d\bar{g}_2 T}{\mu^2}} \right). \tag{38}$$

To investigate the meaning of this equation, let us focus on the case $\mu > 0$, in which the previous equation can be solved as:

$$\kappa(t) \rightarrow \mu \frac{\sqrt{1 + \frac{2d\bar{g}_2 T}{\mu^2}} - 1}{2d\bar{g}_2}. \tag{39}$$

Now let us consider the equilibrium distribution. The melonic equilibrium solution can be investigated from the standard methods in RTM literature [12] using Schwinger-Dyson equations, which we recall briefly here in this context for self-consistency. The partition function of the equilibrium state reads:

$$Z_{\text{eq}} := \int d\mathbf{T} d\bar{\mathbf{T}} e^{-2\mathcal{H}[\mathbf{T}\bar{\mathbf{T}}]/T}, \tag{40}$$

where $d\mathbf{T} d\bar{\mathbf{T}} := \prod_{i_1, \dots, i_d} dT_{i_1 \dots i_d} d\bar{T}_{i_1 \dots i_d}$ is the standard Lebesgue measure, and \mathbf{T} is now time independent. Let us consider the Schwinger-Dyson equation:

$$0 = \sum_I \int d\mathbf{T} d\bar{\mathbf{T}} \frac{\partial}{\partial T_I} \left(T_I e^{-2\mathcal{H}[\mathbf{T}\bar{\mathbf{T}}]/T} \right). \tag{41}$$

Computing the derivative, and dividing the resulting equation by $N^d Z_{\text{eq}}$, we arrive to the equation:

$$1 - \frac{2\mu}{T} Q - \frac{2d\bar{g}_2}{T} Q^2 \asymp 0, \tag{42}$$

where Q is defined as:

$$Q := \frac{1}{N^d} \frac{1}{Z_{\text{eq}}} \int d\mathbf{T} d\bar{\mathbf{T}} \left(\sum_I \bar{T}_I T_I \right) e^{-2\mathcal{H}[\mathbf{T}\bar{\mathbf{T}}]/T}, \tag{43}$$

and used of the large N self averaging condition [13]:

$$\frac{1}{N^d Z_{\text{eq}}} \int d\mathbf{T} d\bar{\mathbf{T}} \mathcal{V}_c[\mathbf{T}, \bar{\mathbf{T}}] e^{-2\mathcal{H}[\mathbf{T}\bar{\mathbf{T}}]/T} \asymp \sum_{p \geq 1} \frac{\bar{g}_p}{p} Q^p. \tag{44}$$

The solution of (42) is:

$$Q = \mu \frac{\sqrt{1 + \frac{2d\bar{g}_2 T}{\mu^2}} - 1}{2d\bar{g}_2}, \tag{45}$$

where we selected only the solution that goes toward $T/2\mu$ as \bar{g}_2 vanishes. This shows that $\kappa(t) \rightarrow Q$ for large t , and that the system goes toward the equilibrium regime described by the equilibrium state (6). Note that equilibrium solution (45) is defined below the critical value:

$$g_c = -\frac{\mu^2}{2dT}, \tag{46}$$

at which the free energy $f_{\text{eq}} := \ln Z_{\text{eq}}$ becomes non-analytic,

$$f_{\text{eq}} \sim |g - g_c|^{3/2} =: |g - g_c|^{2-\theta} \tag{47}$$

corresponding to the entropy exponent $\theta = 1/2$. Finally, note that the leading order Schwinger Dyson equation means that:

$$2U'(\kappa) = \frac{T}{\kappa} = \max(i\omega_{\pm}), \tag{48}$$

hence, $G(t) \sim e^{(T/\kappa)t}$ rather than $e^{(T/r_0)t}$.

3.3. Low temperature regime

The result can be generalized for potentials of the form:

$$U'(\kappa) = \frac{1}{2}(\kappa - \gamma)R(\kappa), \tag{49}$$

where the zeros of the function $R(\kappa)$ are assumed to be different and far enough to the isolated zero $\kappa = \gamma$. If the system is found initially in the vicinity of the isolated zero, and if we assume that the system converges toward some equilibrium value κ_{∞} for late time, close enough to the value $\kappa = \gamma$ (see also Section 4, paragraph b), the equation for \dot{G} reads approximately:

$$\dot{G} \approx G(t) \left(\frac{\Delta + T \int_0^t dt' G(t')}{G(t)} - \gamma \right) R(\kappa_{\infty}), \tag{50}$$

which can be solved again as a combination of exponential with:

$$i\omega_{\pm} = R(\kappa_{\infty}) \frac{\gamma}{2} \left(\pm \sqrt{1 + \frac{4T}{\gamma^2 R(\kappa_{\infty})}} - 1 \right) \tag{51}$$

The late time behavior corresponds to the $\min i\omega_{\pm}$, and the equation fixing the value of κ_{∞} is:

$$R(\kappa_{\infty}) \frac{\gamma}{2} \left(\sqrt{1 + \frac{4T}{\gamma^2 R(\kappa_{\infty})}} - 1 \right) = (\kappa_{\infty} - \gamma)R(\kappa_{\infty}), \tag{52}$$

which can be rewritten as:

$$\kappa_{\infty}(\kappa_{\infty} - \gamma)R(\kappa_{\infty}) = T, \tag{53}$$

which is nothing but the leading order Schwinger Dyson equation for large N .

It seems that the ability of the system to reach the equilibrium distribution depends strongly on the shape of the potential. As an example, let us investigate the case of a potential with twice degenerate vacua:

$$\frac{\partial U(\kappa)}{\partial \kappa} = \frac{1}{2}(\kappa - \gamma)^2. \tag{54}$$

The equation for \dot{G} reads:

$$\dot{G} = G \left(\frac{\Delta + T \int_0^t dt' G(t')}{G(t)} - \gamma \right)^2 \tag{55}$$

Because G is positive, the right-hand side is positive at all times, and G can only grow over time. For T small enough, one can expand the right-hand side up to linear order in T , and for late time, one can neglect Δ/G with respect to contributions of order G^0 and G^1 . We have:

$$\dot{G} = \left(\gamma^2 G(t) - 2\gamma T \int_0^t G(t') dt' + 2\Delta \left(T \frac{\int_0^t G(t') dt'}{G(t)} - \gamma \right) \right). \tag{56}$$

Assuming that $G(t)$ expands in power series of T :

$$G(t) = \sum_{n=0}^{\infty} T^n G_n(t), \tag{57}$$

we get for G_0 :

$$G_0(t) = C_0 e^{\gamma^2 t} + \frac{2\Delta}{\gamma}. \tag{58}$$

In the same way, the equation for $G^{(1)}$ reads:

$$\dot{G}_1 = \gamma^2 G_1 - 2\gamma \int_0^t G_0(t') dt' + 2\Delta \frac{\int_0^t G_0(t') dt'}{G_0(t)}, \tag{59}$$

which can be solved as:

$$G_1(t) = \left(C_1 - 2 \int_0^t dt' \int_0^{t'} dt'' G_0(t'') \left[\gamma - \frac{\Delta}{G_0(t')} \right] \right) e^{\gamma^2 t}. \tag{60}$$

The numerical constants C_1 and C_0 will be fixed by the initial condition $G(0) = 1$, leading to:

$$C_0 + T C_1 + \frac{2\Delta}{\gamma} = 1 \tag{61}$$

and $G(t)$ reads:

$$G(t) = e^{\gamma^2 t} \left(\left(1 - \frac{2\Delta}{\gamma} \right) - 2T \int_0^t dt' e^{-\gamma^2 t'} \int_0^{t'} dt'' G_0(t'') \left[\gamma - \frac{\Delta}{G_0(t')} \right] \right). \tag{62}$$

For a later time, the right-hand side can be computed exactly, and we have:

$$G(t) \approx e^{\gamma^2 t} \left(\left(1 - \frac{2\Delta}{\gamma} \right) - 2T \left(\frac{A}{12\gamma^4 \Delta} + \frac{1 - 2\Delta/\gamma}{\gamma} t \right) \right), \tag{63}$$

where:

$$\begin{aligned}
 A := & \Delta \left((\pi^2 - 6) \gamma - 2 (\pi^2 - 12) \Delta \right) + 6\Delta(\gamma - 2\Delta)\text{Li}_2 \left(1 - \frac{\gamma}{2\Delta} \right) \\
 & + 3(\gamma - 2\Delta) \left(\Delta \log^2 \left(\frac{\gamma}{2\Delta} - 1 \right) + \gamma \log \left(1 - \frac{2\Delta}{\gamma} \right) \right), \tag{64}
 \end{aligned}$$

where $\text{Li}_s(z)$ is the standard poly-logarithm function. Computing the first derivative with respect to t , a straightforward calculation leads to³:

$$\frac{\dot{G}}{G} \approx \gamma^2 - \frac{2T}{\gamma} + \mathcal{O}(T^2). \tag{65}$$

Hence, for T small enough, the asymptotic equation fixing κ is:

$$\gamma^2 - \frac{2T}{\gamma} \approx (\kappa - \gamma)^2, \tag{66}$$

which have two solutions:

$$\kappa = \frac{T}{\gamma^2}, \quad \text{or} \quad \kappa = 2\gamma - \frac{T}{\gamma^2}. \tag{67}$$

In contrast, the leading order Schwinger Dyson equation for the equilibrium theory reads:

$$QU'(Q) = T, \tag{68}$$

which, for small T solves as:

$$Q \approx \gamma \pm \sqrt{\frac{T}{\gamma}}, \quad \text{or} \quad Q \approx \frac{T}{\gamma^2}. \tag{69}$$

This result shows that, at least for T small enough, equilibrium dynamics selects only one of the three solutions of the equilibrium distribution, the vacuum such that $Q = \mathcal{O}(T)$. One can expect that this concerns only zeros with even degeneracy, but a simple argument shows that it concerns odd potential as well. To show this, let us consider the potential:

$$\dot{G} = G(t) \left(\frac{\Delta + T \int_0^t dt' G(t')}{G(t)} - \gamma \right)^n. \tag{70}$$

In contrast with the previous case, the right-hand side is not positive, and one may expect that the equation converges toward a finite value, say κ_∞ . Hence, assuming the system is closed to this limit:

$$\kappa(t) = \kappa_\infty + \varepsilon(t). \tag{71}$$

At first order in $\varepsilon(t)$, we have:

$$\dot{G} = n(\kappa_\infty - \gamma)^{2n} \left(\Delta + T \int_0^t dt' G(t') - \kappa_\infty G(t) \right), \tag{72}$$

corresponding to the frequencies:

³ The computation requires that t remains not too large, $t \lesssim T/\gamma$.

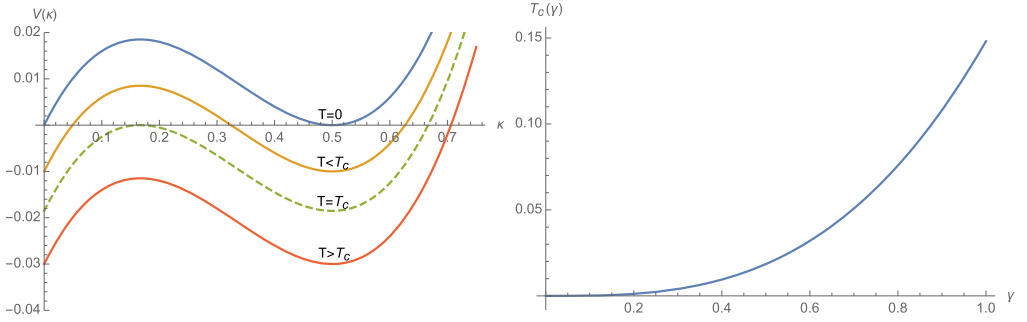


Fig. 2. Shape of the potential $V(\kappa)$ for some temperature above and below the critical temperature with $\gamma = 0.5$ and critical temperature dependency on γ .

$$i\omega_{\pm} = n(\kappa_{\infty} - \gamma)^{2n} \frac{\kappa_{\infty}}{2} \left(\pm \sqrt{1 + \frac{4T}{\kappa_{\infty}^2 n(\kappa_{\infty} - \gamma)^{2n}} - 1} \right). \tag{73}$$

For late time, the equation for κ_{∞} can be rewritten as:

$$\kappa_{\infty} i\omega_{+} \approx T, \tag{74}$$

which matches with the leading order Schwinger Dyson equation for T small enough. Hence, these simple arguments seem to indicate that potentials having degenerate zeros converge toward equilibrium for late time, i.e. the asymptotic probability distribution agrees with the predictions of the equilibrium distribution (6) for T small enough. In the next section, we confirm these statements with numerical simulations for the late-time behavior.

3.4. Numerical study

The equation for \dot{G} can be investigated numerically. In this section, we focus on the case of purely degenerate vacua, of the form (70). First, let us consider the quadratic case. If equilibrium is reached, the leading contribution to $G(t)$ for a late time has to behave as⁴:

$$G(t) \sim \alpha \exp\left(\frac{T}{\kappa_{\infty}} t\right), \tag{76}$$

where κ_{∞} is a zero of the potential $V(\kappa) := \kappa(\kappa - \gamma)^2 - T$. There are two regimes, depending on the temperature. For $T < T_c(\gamma)$, there are three real zeros, and for $T \ll 1$ these zeros display as equation (69) shows, with a zero of order T and two zeros of order γ . For $T > T_c(\gamma)$ in contrast, the potential has only one real zero, identified from continuity with T as the larger zero among the three real zeros occurring from the low-temperature regime. Fig. 2 shows the behavior of the potential $V(\kappa)$ and $T_c(\gamma)$, which is explicitly given by:

⁴ Let $G(t) = A e^{Bt}$. Assuming t large enough, $G(t)$ is a solution of the equation of motion if:

$$B = \left(\frac{T}{B} - \gamma\right)^n. \tag{75}$$

Hence, if $B = T/\kappa_{\infty}$, the equation reads $\kappa_{\infty}(\kappa_{\infty} - \gamma)^n = T$, which is nothing but the leading order Schwinger Dyson equation.

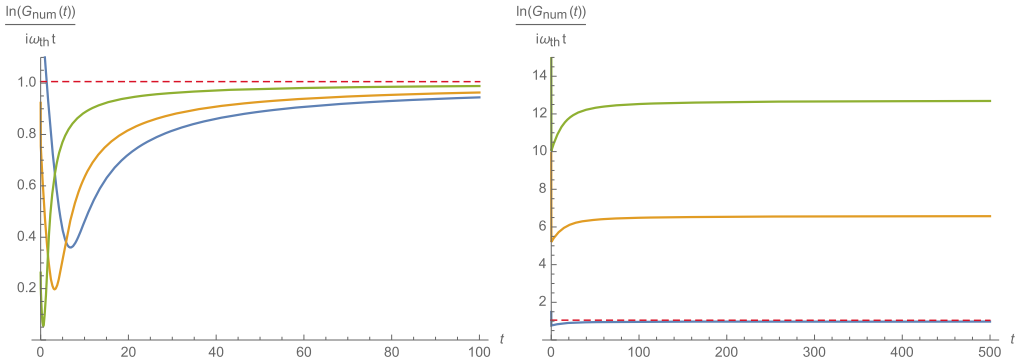


Fig. 3. Behavior of $\ln G_{\text{num}}/(i\omega_{\text{th}}t)$ respectively for $T > T_c$ (on the left) and for $T < T_c$ (on the right).

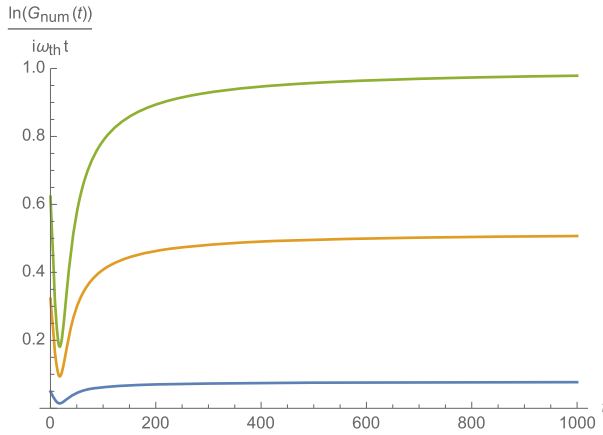


Fig. 4. Behavior of $\ln G_{\text{num}}/(i\omega_{\text{th}}t)$ below the critical temperature for $\Delta = 0.4$ and $\gamma = 0.5$.

$$T_c(\gamma) = \frac{4\gamma^3}{27}. \tag{77}$$

Let us denote as G_{num} the numerical solution of equation (70) for $n = 2$. Fig. 3 shows the behavior of $\ln(G_{\text{num}}(t))/(i\omega_{\text{th}}t)$ above and below the critical temperature $T_c \approx 0.019$ for $\gamma = 0.5$ and $\Delta = 0.1$, the theoretical value $i\omega_{\text{th}}$ being equals to T/κ_∞ , such that $V(\kappa_\infty) = 0$. As we can show on the Fig. 3 for $T = 0.1, 0.2$ and 1 , $G_{\text{num}}(t) \sim e^{i\omega_{\text{th}}t}$ for t large enough. The same thing occurs below the critical temperature, and the second diagram in Fig. 3 shows the behavior of $\ln(G_{\text{num}}(t))/(i\omega_{\text{th}}t)$ for $T = 0.01$ for each of the three solutions of the equation $V(\kappa_\infty) = 0$. Among the three solutions, only one converges to 1 for late time, the closed one to the initial condition $\kappa(t = 0) = \Delta$. Fig. 4 illustrates how the system flips between the two stable vacua (i.e. the smallest and the largest), for $\Delta = 0.4$. Colors have the same meaning in Fig. 3 and 4: the blue curve corresponds to the smallest zero $\kappa_\infty \approx T/\gamma$ and the green curve to the largest zero $\kappa_\infty \approx \gamma + \sqrt{T/\gamma}$. For $\Delta = 0.1$ the system reaches the smallest vacuum, and for $\Delta = 0.4$ the system reaches the larger vacuum.

After a transition regime, the relaxation toward equilibrium can be numerically investigated, and, indeed:

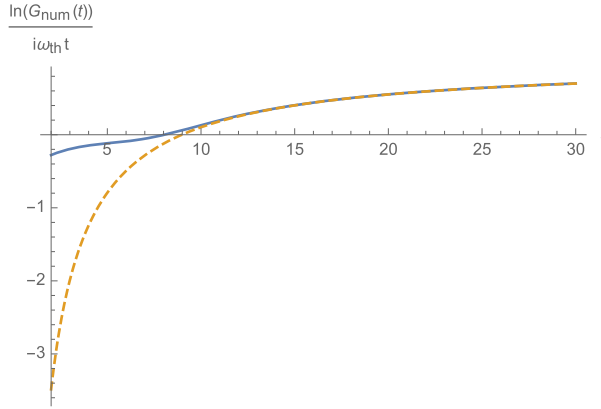


Fig. 5. Behavior of $\ln(G_{\text{num}}(t))/(i\omega_{\text{th}}t)$ for $n = 3$. The dotted edge corresponds to $f(t) := 1 - 8.9682/t$.

$$\frac{\ln(G_{\text{num}})}{i\omega_{\text{th}}t} \sim 1 - \frac{\alpha}{t}. \tag{78}$$

Similar behavior is observed for $n > 2$. In general, there are a positive and a negative zero for $V(\kappa)$, and the value toward which $\ln(G_{\text{num}}(t))/(i\omega_{\text{th}}t)$ converges is compatible with Schwinger-Dyson equation for equilibrium state. Fig. 5 shows the behavior of $\ln(G_{\text{num}}(t))/(i\omega_{\text{th}}t)$ for $\Delta = 0.1$, $\gamma = 0.5$ and $T = 0.1$. Numerically, the system reaches the equilibrium state and:

$$G_{\text{num}}(t) \sim 0.396 \exp(0.103t). \tag{79}$$

Remark 1. The assumption (16) can be easily justified along the dynamics from the following argument. Let us compute $\dot{\lambda}_\mu$, the rate of the μ -th eigenvalue of $(\Phi_c)_{ij}$. Because Φ_c is hermitian, it has N real eigenvalues and admits N normalized and orthogonal eigenvectors $\{u_i^{(\mu)}\}$, $\mu \in \llbracket 1, N \rrbracket$, such that:

$$\sum_{j=1}^N (\Phi_c)_{ij} u_j^{(\mu)} = \lambda_\mu u_i^{(\mu)}. \tag{80}$$

It is easy to check that:

$$\begin{aligned} \sum_{i,j=1}^N u_i^{(\mu)} u_j^{(\mu)} (\dot{\Phi}_c)_{ij} &= \dot{\lambda}_\mu - \lambda_\mu \frac{d}{dt} \sum_{i=1}^N u_i^{(\mu)} u_i^{(\mu)} \\ &= \dot{\lambda}_\mu - \lambda_\mu \frac{d}{dt} 1 \equiv \dot{\lambda}_\mu. \end{aligned} \tag{81}$$

The rate $\dot{\lambda}_\mu$ has then the general structure:

$$\dot{\lambda}_\mu = F_\mu, \tag{82}$$

where F_μ is the projection of the right-hand side of the Langevin equation. Now, let us investigate the large N distribution $P_0(\vec{\Phi}_0)$ for the initial distribution of $\Phi_{0,c} := \Phi_c(t = 0)$, where $\vec{\Phi}_0 := \{\Phi_{0,c}\}$. Because (22), we have:

$$\langle (\Phi_{0,c})_{ij} \rangle_0 = N^{d-1} \Delta \delta_{ij}. \tag{83}$$

Computing the 2-point correlation, we have:

$$\langle\langle\Phi_{0,c}\rangle_{ij}\langle\Phi_{0,c}\rangle_{kl}\rangle_0 = \langle\langle\Phi_{0,c}\rangle_{ij}\rangle_0\langle\langle\Phi_{0,c}\rangle_{kl}\rangle_0 + \langle\langle\Phi_{0,c}\rangle_{ij}\langle\Phi_{0,c}\rangle_{kl}\rangle_{0,C}, \tag{84}$$

where the last piece is the connected contribution, which can be easily computed from (22). This leads to:

$$\begin{aligned} \langle\langle\Phi_{0,c}\rangle_{ij}\langle\Phi_{0,c}\rangle_{kl}\rangle_{0,C} &= \Delta^2 \sum_{I/c, J/c} \delta_{I/c} \delta_{J/c} \delta_{il} \delta_{jk} \\ &= N^{d-1} \Delta^2 \delta_{il} \delta_{jk}, \end{aligned} \tag{85}$$

where $I/c \in \llbracket 1, N \rrbracket^{d-1}$ includes all indices excepts the one of color c . The connected contribution is sub-leading (with a factor $1/N^{d-1}$) concerning the disconnected piece, and in the large N limit we have:

$$\langle\langle\Phi_{0,c}\rangle_{ij}\langle\Phi_{0,c}\rangle_{kl}\rangle_0 \simeq \langle\langle\Phi_{0,c}\rangle_{ij}\rangle_0\langle\langle\Phi_{0,c}\rangle_{kl}\rangle_0. \tag{86}$$

In the same way to find:

$$\langle\prod_{\ell=1}^N \langle\Phi_{0,c}\rangle_{i_\ell j_\ell}\rangle_0 \simeq \prod_{\ell=1}^N \langle\langle\Phi_{0,c}\rangle_{i_\ell j_\ell}\rangle_0, \tag{87}$$

and the probability P_0 , at leading order in N corresponds to a delta-distribution:

$$P_0(\vec{\Phi}_0) \asymp \prod_{c=1}^d \delta(\langle\Phi_0\rangle_c - N^{d-1} \Delta \text{Id}), \tag{88}$$

where Id is the $N \times N$ identity matrix. At the initial time, the distribution is localized around a diagonal matrix with equal entries. Hence, in the rate equation for $\dot{\lambda}_\mu$, initial conditions are the same for all eigenvalues, and they remain identical for all time. The argument easily generalizes for $D > 0$.

4. Blank noise limit for $D > 0$: UV regularized theory below critical temperature

For $D > 0$, the Laplacian contribution in equation (1) modifies the effective large N dynamics given by equation (19) as follows:

$$\dot{T}_{i_1 \dots i_d} = -T_{i_1 \dots i_d} U'(\kappa) + \partial_x^2 T_{i_1 \dots i_d} + \eta_{i_1 \dots i_d}. \tag{89}$$

Hence, κ self averages again, but an additional contribution arises because of the Laplacian term. This equation can be formally solved using Fourier transform, with the convention:

$$T_{i_1 \dots i_d}(x, t) =: \int_{-\infty}^{+\infty} \frac{dk}{(2\pi)^{D/2}} \mathcal{T}_{i_1 \dots i_d}(k, t) e^{ik \cdot x}, \tag{90}$$

where $k \in \mathbb{R}^D$ and “ $u \cdot v$ ” is the standard scalar product. Hence, assuming again that Φ_c self averages for large N around a diagonal matrix which is independent of c , and the dynamical equation can be easily solved after they quench as:

$$\mathcal{T}_{i_1 \dots i_d}(k, t) = \mathcal{T}_{i_1 \dots i_d}(k, 0)\rho(k, t) + \int_0^t dt' \eta_{i_1 \dots i_d}(k, t') \frac{\rho(k, t)}{\rho(k, t')}, \tag{91}$$

with:

$$\rho(k, t) := e^{-k^2 t - g(t)}, \quad g(t) := \int_0^t dt' U'(\kappa(t')), \tag{92}$$

and the initial correlation in the Fourier space reads:

$$\langle \bar{\mathcal{T}}_{i_1 \dots i_d}(k, 0) \mathcal{T}_{j_1 \dots j_d}(k', 0) \rangle_0 = \Delta \prod_{c=1}^d \delta_{i_c j_c} e^{-\frac{k^2}{2\Lambda^2}} \delta(k - k'). \tag{93}$$

From (161) and (93), the equation for $r(t)$ becomes:

$$r(t) = \Delta \int_{-\infty}^{+\infty} \frac{dk}{(2\pi)^{D/2}} e^{-2k^2(t+\tau) - 2g(t)} + T \int_0^t dt' \int_{-\infty}^{+\infty} \frac{dk}{(2\pi)^{D/2}} e^{-2k^2(t-t'+\tau)} e^{-2(g(t) - g(t'))}, \tag{94}$$

where:

$$\tau := \frac{1}{4\Lambda^2}. \tag{95}$$

We will consider firstly the quartic case because the closed equation can be solved asymptotically using Laplace transform. This in particular shows the existence of a critical temperature, which is finite in contrast to the zero-dimensional model. We then consider the general cases using a low temperature expansion, where transition temperature looks as the radius of convergence of the series.

4.1. The quartic case

Let us investigate the quartic case. If we assume [2,9] that for t large enough, $U'(\kappa(t)) \rightarrow 0$, the self-consistent equation for $g(t)$ reads:

$$0 \approx \mu + \bar{g}_2 d \left(\Delta \int_{-\infty}^{+\infty} \frac{dk}{(2\pi)^{D/2}} e^{-2k^2(t+\tau) - 2g(t)} + T \int_0^t dt' \int_{-\infty}^{+\infty} \frac{dk}{(2\pi)^{D/2}} e^{-2k^2(t-t'+\tau)} e^{-2(g(t) - g(t'))} \right), \tag{96}$$

that can be rewritten as:

$$G(t) = -\frac{\bar{g}_2 d}{\mu} \left(\Delta H(t) + T F(t) \right), \tag{97}$$

where

$$H(t) := \frac{1}{2^D} \frac{1}{(t + \tau)^{D/2}}, \tag{98}$$

and:

$$F(t) := \int_0^t dt' H(t-t')G(t'). \tag{99}$$

In the zero temperature limit, the problem is then solved and $G(t) \sim 1/t^{D/2}$, and then $U'(\kappa(t)) \sim 1/t$, in agreement with our assumption. Note that $G(t)$ being a positive definite quantity, this makes sense only for $\mu < 0$. Hence, for $t \gg \tau$:

$$\mathcal{T}_{i_1 \dots i_d}(k, t) = \mathcal{T}_{i_1 \dots i_d}(k, 0) \left(-\frac{2^D \mu}{\bar{g}_2 d} \right)^{\frac{1}{2}} t^{D/4} e^{-k^2 t}. \tag{100}$$

The 2-point correlation function for equal times $C(|x|, t) := \sum_I \langle \bar{T}_I(x, t) T_I(0, t) \rangle$ behaves as $\sim e^{-\frac{|x|^2}{8t}}$ for t large enough, and the correlation length grows as \sqrt{t} , meaning that the system does not reach a thermal regime at a finite time.

For $T \neq 0$, one can expect to solve the equation using Laplace transform. Let us denote as $\bar{f}(p)$ the Laplace transform of the function $f(t)$ as:

$$\bar{f}(p) := \int_0^{+\infty} dt f(t) e^{-pt}. \tag{101}$$

The standard properties of Laplace transform regarding the convolution product. We get straightforwardly:

$$\bar{G}(p) = -\frac{\Delta}{T + \frac{\mu}{\bar{g}_2 d} \bar{H}^{-1}(p)}, \tag{102}$$

and the Laplace transform of H can be easily computed as:

$$\bar{H}(p) = 2^{-D} p^{\frac{D}{2}-1} e^{p\tau} \int_{p\tau}^{+\infty} dt t^{-\frac{D}{2}} e^{-t}, \tag{103}$$

and in particular for $D = 3$:

$$\bar{H}(p) = \frac{2 - 2\sqrt{\pi} e^{p\tau} \sqrt{p\tau} \operatorname{erfc}(\sqrt{p\tau})}{8\sqrt{\tau}}. \tag{104}$$

Fig. 6 shows the function $\bar{H}(p)$. Hence, for large t i.e. for small p ,

$$\bar{H}(p) \sim \frac{1}{4\sqrt{\tau}} - \frac{\sqrt{\pi}\sqrt{p}}{4}. \tag{105}$$

Table 1 provides some explicit expressions for low dimensions and their asymptotic behavior for small p . Note that in this table, $\gamma \approx 0.57$ is the Euler constant, erfc is the complement error function and $\operatorname{Ei}(x)$ is the standard exponential integral:

$$\operatorname{Ei}(x) := \int_x^\infty \frac{e^{-t}}{t} dt. \tag{106}$$

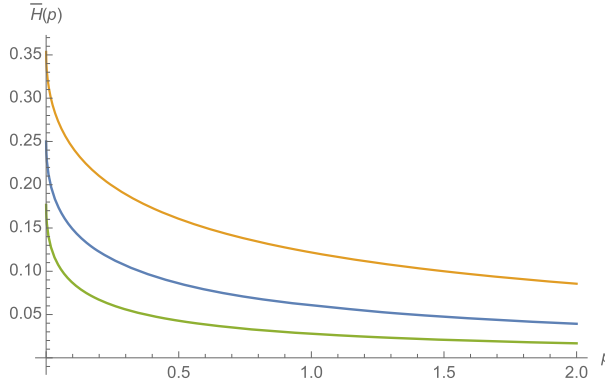


Fig. 6. Shape of $\bar{H}(p)$ for $D = 3$, for $\tau = 1$ (blue curve), $\tau = 0.5$ (yellow curve), and $\tau = 2$ (green curve).

At this stage, we have to clarify a technical point. The closed equation (97) that we considered is only an asymptotic relation. Nevertheless, we integrated it for all time taking the Laplace transform, although the closed equation is expected to be wrong for small times. Indeed, we assume the solution of the closed equation provides the true asymptotic behavior for $G(t)$, which can be motivated by the two following observations:

- For t large enough, $H(t - t')$ suppresses low-time contributions provided that $G(t)$ has a finite limit for short times.
- Fluctuations for $U'(\kappa(t))$ are assumed to have a small standard deviation around the large time-averaged value.

We do the same assumption for higher-order potentials that we will consider in the next section. From Table 1, we show that all the computed values for $\bar{H}(0)$ are non-vanishing, but the sign of this value depends on the dimension and the size of τ . For $D = 1, 2$, $\bar{H}(0) = \infty$, and $\bar{G}(0)$ is non singular. For $D = 3$, $\bar{G}(0)$ is defined for $T < T_c$, with:

$$T_c(D = 3) = -\frac{4\mu}{3\bar{g}_2} \sqrt{\tau}, \tag{107}$$

which vanishes in the limit $\tau \rightarrow 0$ keeping μ/\bar{g}_2 fixed. For $D > 2$, we have:

$$T_c(D) = -\frac{\mu}{\bar{g}_2 d} 2^{D-1} (D - 2) \tau^{\frac{D}{2}-1}. \tag{108}$$

The large time behavior for $G(t)$ can be deduced from the small p expansion of $\bar{G}(p)$. It can be understood from standard theorems on the Laplace transform near the origin [19], and we have for instance the following statement:

Theorem 1. *Let $f(t)$ be a locally integrable function on $[0, \infty)$ such that $f(t) \approx \sum_{m=0}^{\infty} c_m t^{r_m}$ as $t \rightarrow \infty$ where $r_m < 0$. If the Mellin transformation of this function is defined and if no $r_m = -1, -2, \dots$ then the Laplace transformation of $f(t)$ is*

$$\bar{f}(p) = \sum_{m=0}^{\infty} c_m \Gamma(r_m + 1) p^{-r_m-1} + \sum_{n=0}^{\infty} Mf(n + 1) \frac{(-p)^n}{n!} \tag{109}$$

Table 1
Explicit expressions for $\bar{H}(p)$ in low dimension.

D	$\bar{H}(p)$	$p \ll 1$
1	$\frac{\sqrt{\pi} e^{p\tau} \operatorname{erfc}(\sqrt{p\tau})}{2\sqrt{p}}$	$\sim \frac{\sqrt{\pi}}{2\sqrt{p}} - \sqrt{\tau}$
2	$-\frac{1}{4} e^{p\tau} \operatorname{Ei}(-p\tau)$	$\sim \frac{1}{4} (-\log(p\tau) - \gamma) - \frac{1}{4} p(\tau(\log(p) + \log(\tau) + \gamma - 1))$
4	$\frac{1}{16} \left(p e^{p\tau} \operatorname{Ei}(-p\tau) + \frac{1}{\tau} \right)$	$\sim \frac{1}{16\tau} + \frac{1}{16} p(\log(p) + \log(\tau) + \gamma)$
5	$\frac{4\sqrt{\pi} e^{p\tau} (p\tau)^{3/2} \operatorname{erfc}(\sqrt{p\tau}) - 4p\tau + 2}{96\tau^{3/2}}$	$\sim \frac{1}{48\tau^{3/2}} - \frac{p}{24\sqrt{\tau}}$
6	$-\frac{p^2 \tau^2 e^{p\tau} \operatorname{Ei}(-p\tau) + p\tau - 1}{128\tau^2}$	$\sim \frac{1}{128\tau^2} - \frac{p}{128\tau}$

where $Mf(z) = \int_0^\infty t^{z-1} f(t) dt$ is the Mellin transform of the function $f(t)$,

$$Mf(z) := \int_0^\infty ds s^{z-1} f(s). \tag{110}$$

For $D = 3$,

$$\bar{G}(p) \sim \frac{\Delta}{T_c - T} + \frac{\Delta}{(T_c - T)^2} \frac{\mu}{3\bar{g}_2} 4\sqrt{\pi} \sqrt{p\tau} + \mathcal{O}(p), \tag{111}$$

and for $\tau \neq 0$, $T < T_c$, we find that $G(t) \sim t^{-3/2}$. For $D = 4$, the lowest order contribution behaves as $p(\log(p) + \log(\tau) + \gamma)$, and $G(t)$ behaves as $t^{-2} \log(t)$. For $D > 4$, the lowest order in linear with p and $G(t) \sim t^{-2}$. Hence, below the critical dimension, the relaxation time for the zero modes is infinite, and $\langle T_I(0, t) \rangle \sim t^{3/4}$ for $D = 3$. The 2-point temporal correlation function for zero initial time $C(t) \sim \sum_I \langle \bar{T}_I(0, t) T_I(0, 0) \rangle$ behaves as $t^{-3/4}$, and the memory of the system follows a power law. For high temperature in contrast, the previous method breaks down, and we expect that $G(t)$ diverges faster than any power law such that Laplace transform for arbitrary small p does not exist, and the system is expected to forget the initial conditions accordingly with an exponential decays.

4.2. Time evolution and low-temperature expansion

As in section 3, we investigate the time evolution using the definition (24). In replacement of equation (25), we have:

$$\dot{G} = 2\mu G(t) + 2d\bar{g}_2 (\Delta H(t) + TF(t)). \tag{112}$$

Taking Laplace to transform (assuming that Laplace transforms for G exist), we get:

$$\bar{G}(p) = \bar{G}_0(p) + \bar{G}_1(p) \tag{113}$$

with:

$$\bar{G}_0(p) = \frac{1}{p - 2\mu - 2d\bar{g}_2 T \bar{H}(p)}, \tag{114}$$

and

$$\bar{G}_1(p) = \frac{2d\bar{g}_2 \Delta \bar{H}(p)}{p - 2\mu - 2d\bar{g}_2 T \bar{H}(p)}, \tag{115}$$

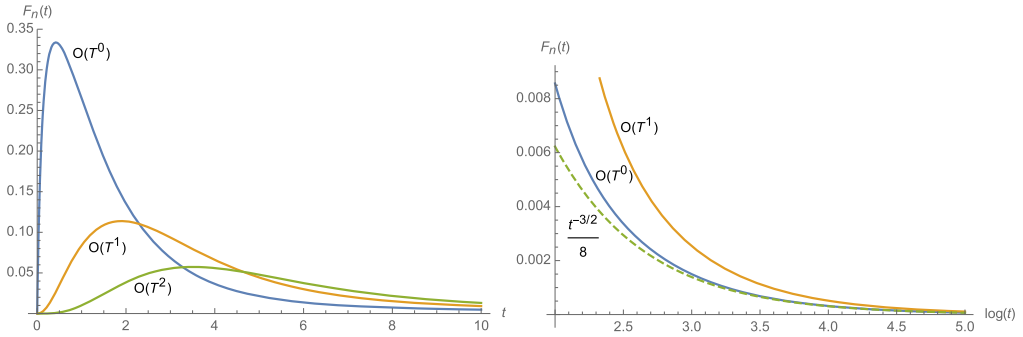


Fig. 7. On the left: Behavior of F_0 (blue curve), F_1 (yellow curve) and F_2 (green curve). On the right: behavior of F_0 and F_1 for late time, compared with the asymptotic behavior for $F_0(t)$ (dotted green curve).

assuming $\mu < 0$, the series expansion in T of $G_1(t)$ leads to:

$$\frac{G_1(t)}{\Delta} = xF_0(t) + x^2TF_1(t) + x^3T^2F_2(t) + \dots \tag{116}$$

where $x := 2d\bar{g}_2$ and:

$$F_0(t) := \int_0^t dt' e^{2\mu(t-t')} H(t'), \tag{117}$$

$$F_n(t) := \int_0^t dt' F_0(t-t')F_{n-1}(t'), \quad n > 0. \tag{118}$$

Fig. 7 shows the behavior of F_0 , F_1 and F_2 for $D = 3$, $2\mu = 1$ and $\tau = 0.1$. Asymptotically, $F_0(t)$ behaves as $1/t^{3/2}$, precisely:

$$F_0(t) \approx \frac{0.125}{t^{3/2}} \tag{119}$$

for t large enough. In the second Figure in Fig. 7 we show the behavior of F_0 and F_1 and the asymptotic behavior $\sim 0.125/t^{3/2}$. The functions $F_n(t)$, for $n > 0$ are also asymptotically uniformly bounded by $a/t^{3/2}$ for some $a > 0$, but we can check numerically that $F_n(t)/t^{3/2} \rightarrow 0$ for long time. Indeed, numerically $F_n(t)/F_{n-1}(t) \rightarrow 0$ as $t \rightarrow \infty$, but remains almost constant for finite but late time, see Fig. 8.

For G_0 , we get:

$$G_0(t) = e^{2\mu t} + xTK_0(t) + (xT)^2K_1(t) + \dots, \tag{120}$$

where:

$$K_n(t) := \int_0^t dt' e^{2\mu(t-t')} F_n(t'). \tag{121}$$

The typical shape of functions K_n is given in Fig. 9. Once again we find $K_0 \sim 1/t^{3/2}$ and $K_n \geq K_{n-1}$ for late time.

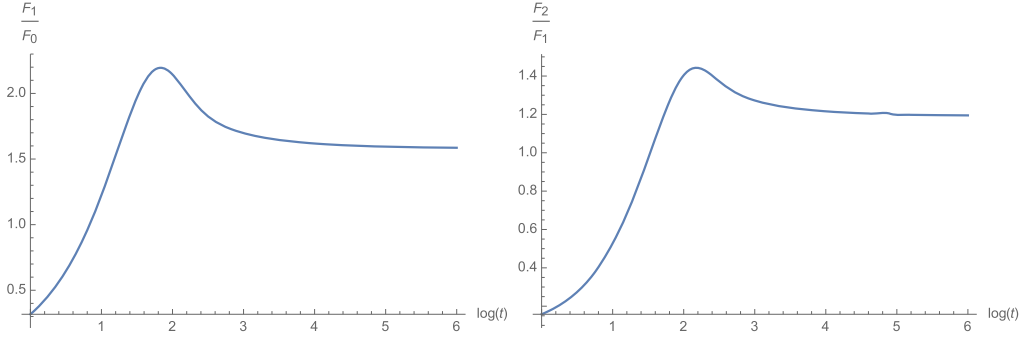


Fig. 8. Asymptotic behavior of F_1/F_0 (on the left) and of F_2/F_1 (on the right) using a logarithmic time scale.

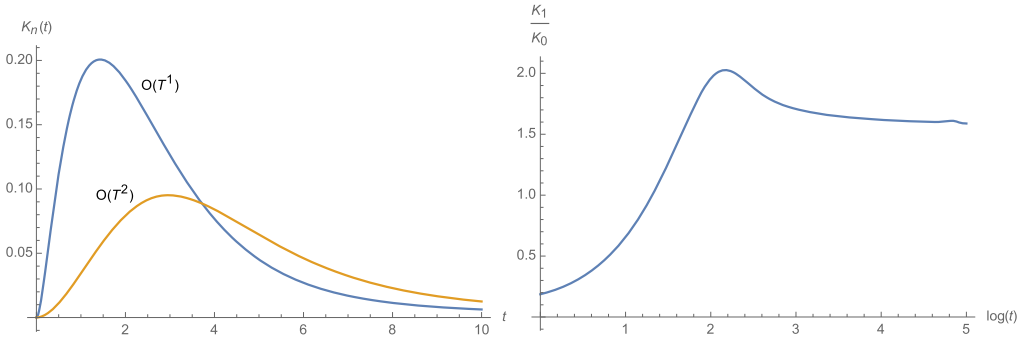


Fig. 9. On the left: behavior of K_0 and K_1 . On the right: the asymptotic behavior of K_1/K_0 for late time using logarithmic scale.

4.3. Continuum limit

All the expressions computed above, and in particular, the transition temperatures vanish for $\Lambda \rightarrow \infty$ i.e. for $\tau \rightarrow 0$, if we keep the fractional μ/\bar{g}_2 fixed. For $D = 3$ for instance, this leads to the inconsistent result:

$$\bar{G}(p) = -\frac{\Delta}{T}, \tag{122}$$

which has the wrong sign because $G(t) = e^{2g(t)}$ is a positive definite quantity. Indeed, one cannot take the continuum limit $\Lambda \rightarrow \infty$ without taking care of the dimensions of couplings. To make a correct dimensional analysis, it is suitable to introduce Ω such that the definitions of the model become:

$$\dot{T}_I(x, t) = -\Omega \frac{\delta \mathcal{H}}{\delta \bar{T}_I(x, t)} + \eta_I(x, t), \tag{123}$$

where the Hamiltonian \mathcal{H} is defined as:

$$\mathcal{H}[T, \bar{T}] := \mathcal{H}[T, \bar{T}] - \sum_I \int d^D x \bar{T}_I(x, t) \partial_x^2 T_I(x, t). \tag{124}$$

The noise distribution furthermore becomes:

$$\langle \eta_{i_1 \dots i_d}(x, t) \bar{\eta}_{j_1 \dots j_d}(x', t') \rangle = \Omega T \prod_{c=1}^d \frac{\delta_{i_c j_c} e^{-\frac{|x-x'|^2}{2\Lambda^{-2}}}}{\Lambda^{-D} (2\pi)^{D/2}} \delta(t-t'). \tag{125}$$

We introduce the bracket notation $[X]$ such that $[dx] = -[\Lambda] = -1$ and we furthermore choose the parameter Ω such that $[T] = 0$. Then, because the equilibrium distribution reads $\text{Exp}(-2\mathfrak{H}/T)$, we must have $[\mathfrak{H}] = 0$, and we straightforwardly deduce that $[\mu] = 2$ and $[\bar{g}_2] = 4 - D$. Finally, from (124), we must have $[t] = -[\Omega] - 2$, and the parameter Ω is nothing but the definition of the timescale. At this step, one can repeat the analysis of the previous subsection to compute the critical temperature. Up to the replacement $H(t) \rightarrow H(t)/\Omega^{D/2}$ and $\tau \rightarrow \tau/\Omega$, it is easy to check that the expression of the critical temperature remains unchanged. Indeed, $\bar{H}(0) \sim \tau^{-\frac{D-2}{2}}$, which provides a factor $\Omega^{\frac{D-2}{2}}$ and therefore exactly compensate the factor $\Omega/\Omega^{D/2}$ arising in front of the term $TF(t)$ in equation (97). Hence, $[\mu/\bar{g}_2] = D - 2$, and the equations have a relevant continuum limit only if the following scaling holds:

$$\frac{\mu}{\bar{g}_2 d} = \kappa_0 \Lambda^{D-2}, \tag{126}$$

where $[\kappa_0] = 0$.

4.4. Higher order potentials

The previous methods cannot be easily generalized for higher-order potentials. Indeed, for a potential of degree m (hence assuming $h_m > 0$ and $G(t) \neq 0$, the closed equation reads in that case:

$$\sum_{k=0}^m h_k (u(t))^k = 0 \tag{127}$$

where:

$$u(t) := \frac{\mathcal{A}(t)}{G(t)}, \tag{128}$$

and:

$$\mathcal{A}(t, G) := \Delta H(t) + TF(t), \tag{129}$$

the function $F(t)$ being defined in (99). Because the coefficients $\{h_k\}$ do not depend on t , equation (127) has only stationary solutions, namely:

$$u(t) = \gamma_\mu, \tag{130}$$

where γ_μ for $\mu \in \llbracket 0, m \rrbracket$ is a real and non-vanishing solution of the equation $\sum_{k=0}^m h_k \gamma^k = 0$. Hence, the asymptotic solutions of equation (127) have to be such that, for large t :

$$\boxed{G_\mu(t) = \frac{\Delta}{\gamma_\mu} H(t) + \frac{T}{\gamma_\mu} \int_0^t H(t-t') G_\mu(t'),} \tag{131}$$

where we included an index μ on G refereeing to the selected zero γ_μ . This equation looks like the equation of an effective quartic model (see equation (97)), and can be solved using Laplace transform again (assuming the Laplace transform for $G(t)$ exists). We have:

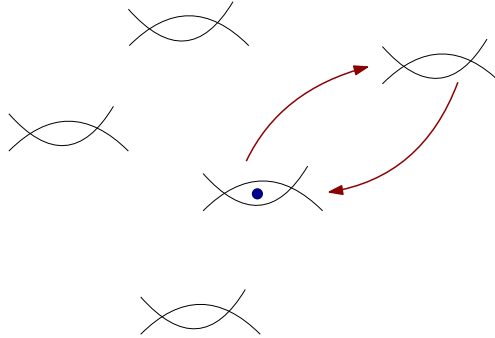


Fig. 10. The system (blue dot) frozen around local extrema for large N , red arrows materialize activation due to thermal fluctuations at finite N .

$$\bar{G}(p) = \frac{\Delta}{\gamma_\mu \bar{H}^{-1}(p) - T}. \tag{132}$$

Because $G(p)$ is positive definite, this solution exists only below the critical temperature:

$$T < T_c^{(\mu)} = \frac{\gamma_\mu}{\bar{H}(0)}. \tag{133}$$

Hence, in the large N limit, each of the vacua is independent of one from the other, without overlapping, and each of them has its critical temperature looking as the radius of convergence of the low-temperature expansion. During its evolution, the system freezes around one of these vacua with a depth of order N^d , and remains around it after an expected short transition period (see Fig. 10). Equation (132) shows that a low temperature expansion for $G(t)$:

$$G(t) =: \sum_{n=0}^{\infty} T^n G^{(n)}(t), \tag{134}$$

where $G^{(n)}(t)$ satisfies the obvious recursive relation:

$$G^{(n)}(p) = T \int_0^t H(t-t') G^{(n-1)}(t'), \quad n > 0, \tag{135}$$

does make sense only below the critical temperature, which looks like the radius of convergence of the series. Note that our derivation assumes the $G(p)$ exists for all p , and especially for small p (i.e. for large t). Hence, the breakdown of the low-temperature expansion is nothing but the manifestation that this assumption for $G(t)$ becomes wrong, and then that a power time behavior leaves its place to an exponential growth i.e. the system relaxes toward equilibrium exponentially in the high-temperature regime. Finally, one expects that activation effects due to thermal fluctuations could play a role for large but finite N (the famous Kramer’s problem) see [26,25,24,21–23]. We investigated these aspects in a forthcoming work.

To conclude this subsection, let us investigate the time evolution, for the quartic model. Following (24), we have:

$$\sum_{k=0}^m h_k(u(t))^k = \frac{1}{2} \frac{\dot{G}}{G}(t). \tag{136}$$

The left-hand side can be factorized around the zeros of the polynomial, then:

$$h_m \prod_{k=0}^m (u(t) - \gamma_k) = \frac{1}{2} \frac{\dot{G}}{G}. \tag{137}$$

Assuming that $u(t)$ is close to some real zero γ_μ , one expects that $|u(t) - \gamma_\mu| \equiv \epsilon(t) \ll 1$, and expanding the left hand side of the previous equation in power of ϵ , we have:

$$\frac{\dot{G}}{G} = 2h_m R(\gamma_\mu)(u(t) - \gamma_\mu)^{\alpha_\mu} + \mathcal{O}(\epsilon^{\alpha_\mu+1}(t)) \tag{138}$$

where α_μ denotes the multiplicity of the zero γ_μ and $R(\gamma_\mu)$ is the remaining contribution evaluated at γ_μ . If we are only interested by the behavior of the system around γ_μ , it is suitable to choose the normalization such that $R(\gamma_\mu) = 1/2h_m$, and

$$\dot{G}(t) \approx G(t)(u(t) - \gamma_\mu)^{\alpha_\mu}. \tag{139}$$

For $\alpha_\mu = 1$, we recover exactly the analysis of the quartic case, and the system behaves as the other zeros were blinded despite thermal fluctuations. For $\alpha_\mu > 1$, the equation can be investigated numerically. Indeed, for $\alpha_\mu = 2$ and as for the $D = 0$ case, $G(t)$ is an increasing function. For $T = 0$, the function converges indeed exponentially as Fig. 12 shows, and we have again:

$$\frac{\ln(G_{\text{num},0}(t))}{t} = \gamma_\mu^2 \left(1 - \frac{\alpha}{t}\right), \tag{140}$$

where the index 0 allows us to recall that $T = 0$, and for $\gamma_\mu = 0.5$, we get for instance $\alpha \approx 0.216$. Hence for $\alpha_\mu = 2$, $G(t)$ behaves exponentially for large t : $G(t) \sim e^{\gamma_\mu^2 t}$, such that the equilibrium regime reduces to the equation (setting $h_m = 1/2$):

$$(\kappa_\infty - \gamma_\mu)^2 = \gamma_\mu^2, \tag{141}$$

and we have two solutions, $\kappa_\infty = 0$ and $\kappa_\infty = 2\gamma_\mu$, meaning that the systems converge towards the zero vacuum due to spatial fluctuations. This obviously contrast with the $T = 0$ limit for $\alpha_\mu = 1$, where $G(t) \sim 1/t^{3/2}$ and $\kappa \rightarrow \gamma_\mu$. For T small enough furthermore, the low T expansion for $G(t)$ shows that the exponential law holds for large t . Indeed, because:

$$\int_0^t dt' H(t-t') e^{a^2 t'} \sim a e^{a^2(\tau+t)} \Gamma\left(-\frac{1}{2}, a^2 \tau\right), \tag{142}$$

where $\Gamma(n, z)$ is the standard incomplete gamma function:

$$\Gamma(n, z) := \int_z^\infty dx x^{n-1} e^{-x}, \tag{143}$$

the solution $G(t) = e^{B^2 t}$ solves the asymptotic equation for \dot{G} provided that B satisfies the transcendental equation: $B^2 = Q(B)$, with

$$Q(B) := \left(T B e^{B^2 \tau} \Gamma\left(-\frac{1}{2}, B^2 \tau\right) - \gamma_\mu \right)^2. \tag{144}$$

The equation can be solved graphically and exhibits generally a single solution, as shown in Fig. 11.

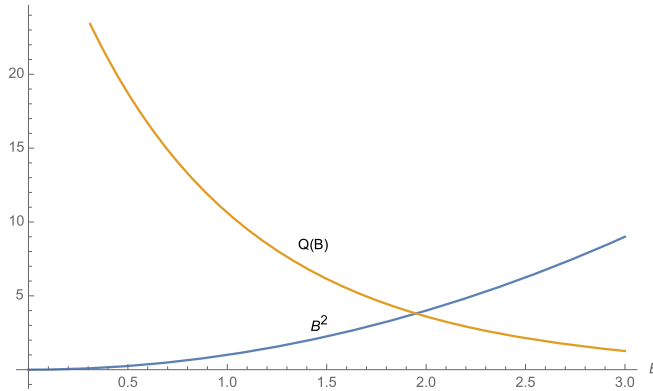


Fig. 11. Graphical solution of the equation $B^2 = Q(B)$ for $\tau = 0.1$ and $\gamma_\mu = 0.5$ ($T=1$).

Note that for γ_μ large enough, and because for large B :

$$\Gamma\left(-\frac{1}{2}, B^2\tau\right) \approx \frac{\exp(-B^2\tau)}{(B^2\tau)^{3/2}}, \tag{145}$$

we have: $B^2 = \gamma_\mu^2(1 + \mathcal{O}(T\gamma_\mu^{-3}))$.

The transition temperature can be estimated from the following argument. Assuming $G(t) = \mathcal{A}(t) e^{\gamma_*^2 t}$ such that $\gamma_*^2 = Q(\gamma_*)$, one gets an equation for $\dot{\mathcal{A}}$:

$$\dot{\mathcal{A}} = \mathcal{A}(t)(u^2(t) - 2\gamma_\mu u(t) + \delta\gamma_\mu^2), \tag{146}$$

where $\delta\gamma_\mu^2 := \gamma_\mu^2 - \gamma_*^2$. Hence as we just discussed, for T small enough in that limit, $u(t)$ is expected to be small for late time, and we can neglect $u^2(t)$, so that the equation reads:

$$\dot{\mathcal{B}} \simeq -2\gamma_\mu e^{-\gamma_\mu^2 t} \left(\Delta H(t) + T \int_0^t H(t-t') \mathcal{B}(t') e^{\gamma_\mu^2 t'} \right), \tag{147}$$

where $\mathcal{B}(t) := \mathcal{A}(t) e^{-\delta\gamma_\mu^2 t}$. The equation can be solved recursively, or by Laplace transform, which leads:

$$\bar{\mathcal{B}}(p) \simeq \frac{1 - 2\gamma_\mu \Delta \bar{H}(p + \gamma_\mu^2)}{p + 2\gamma_\mu T \bar{H}(p + \gamma_\mu^2)}, \tag{148}$$

where $\bar{\mathcal{B}}(p)$ denotes the Laplace transform of $\mathcal{B}(t)$ and we used $\mathcal{B}(t=0) = 1$. For small p , this corresponds to an exponential decay:

$$\mathcal{B}(t) \sim e^{-2\gamma_\mu T \bar{H}(\gamma_\mu^2) t}, \tag{149}$$

and the assumption $\kappa(t) \rightarrow 0$ for large t requires:

$$T < T_c \approx \frac{\gamma_\mu}{2\bar{H}(\gamma_\mu^2)}. \tag{150}$$

The same kind of investigation can be performed for other values of α_μ . Fig. 13 shows the typical behavior of $G_{\text{num},0}(t)$ (for $T = 0$) for $\alpha_\mu = 3$, $\gamma_\mu = 0.5$ and $\Delta = 1$. The evolution starts

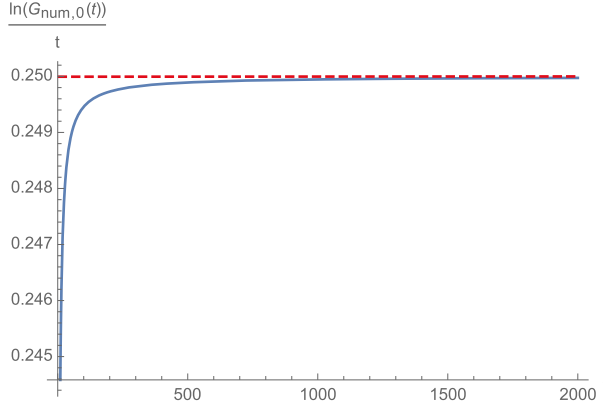


Fig. 12. Evolution of $\ln(G_{\text{num},0}(t))/t \sim 0.25 - 0.054/t$ with $\Delta = 0.1$, $h_m = 1/2$ and $\gamma = 0.5$ for $\alpha_\mu = 2$.

with an exponential phase, $G_{\text{num},0}(t) \sim e^{-\gamma_\mu^3 t}$ for a small time, and ends with a power law decay $G_{\text{num},0}(t) \sim t^{-3/2}$ for late time. Hence, because of the convolution property,

$$\int_0^t \frac{1}{(t-t'+\tau_1)^{\frac{3}{2}}} \frac{1}{(t'+\tau_2)^{\frac{3}{2}}} \sim \left(\frac{1}{\sqrt{\tau_1}} + \frac{1}{\sqrt{\tau_2}} \right) \frac{2}{t^{3/2}}, \tag{151}$$

one expects that for t large enough, $G_{\text{num}}(t) \sim t^{-3/2}$, as for the case $\alpha_\mu = 1$. From this observation, the late time evolution can be investigated from the same method as discussed in section 3.3. In particular, one can estimate the transition temperature from the following argument. During the exponential phase, the system could be close to the zero vacuum, $\kappa \sim 0$. Hence, we find for $G(t)$:

$$\dot{G} \approx -\gamma_\mu^3 G(t) + 3\gamma_\mu^2 \left(\Delta H(t) + T \int_0^t H(t-t')G(t') \right), \tag{152}$$

that can be solved using Laplace transform as:

$$\bar{G}(p) = \frac{1 + 3\gamma_\mu^2 \Delta \bar{H}(p)}{p + \gamma_\mu^3 - T \bar{H}(p)}. \tag{153}$$

Hence, the system ends in the non-zero vacuum γ_μ as $1/t$, provided that $T < T_c \approx \gamma_\mu^3 / \bar{H}(0)$. Note that in this section we provided some estimations for critical temperature, but we do not prove a bound for it, an issue that should be considered in a forthcoming work.

5. Disordered Langevin dynamics

A way to avoid the difficulty arising from UV divergences without taking care of the definition of the continuum limit is to replace the Laplacian in (1) by a disorder coupling, materialized by a random hermitian Wigner matrix $D = D^\dagger$ of size $N^{2 \times d}$:

$$\dot{T}_I(t) = -\frac{\partial \mathcal{H}}{\partial T_I} - \sum_{J \in \llbracket 1, N \rrbracket^d} D_{IJ} T_J(t) + \eta_I(t), \tag{154}$$

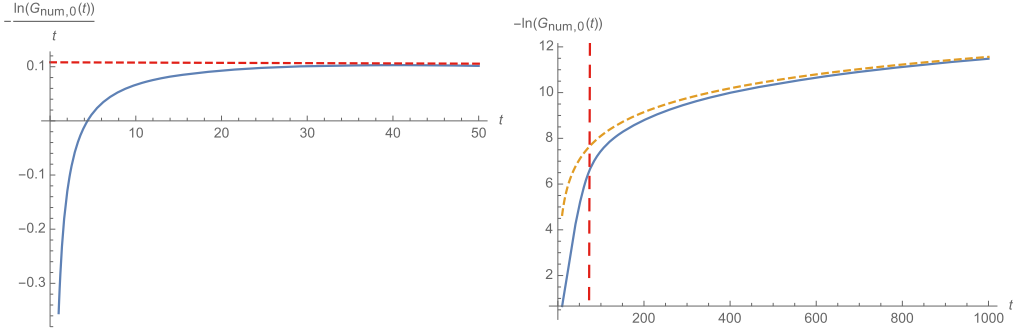


Fig. 13. Typical behavior of $G_{\text{num},0}(t)$ for $T = 0$. On the left for a small time and on the right for a later time. The dotted edge on the top corresponds to the function $f(t) = 1.2 + (3/2)\ln(t)$.

where $T_I \equiv T_I(t)$ i.e. $D = 0$ in this section. We assume that the random matrix D decomposes along each color as a sum of tensorial products:

$$D = \sum_{c=1}^d \mathbb{1}^{\otimes c-1} \otimes \sigma_c \otimes \mathbb{1}^{\otimes d-c-1}, \tag{155}$$

where σ_c 's are hermitian Wigner matrices, which can be formally diagonalized as:

$$\sum_{j=1}^N (\sigma_c)_{ij} u_j^{(\lambda)} = \lambda u_i^{(\lambda)}, \tag{156}$$

where $\{u_i^{(\lambda)}\}$ are orthogonal and normalized. We assume that $\sigma_c \in \text{GUE}$ are centered gaussian matrices with the same variance μ . Hence, in the large N limit, the empirical distribution for eigenvalues converges toward the Wigner law:

$$\frac{1}{N} \sum_{\lambda} f(\lambda) \rightarrow \int_{-2\sigma}^{2\sigma} d\lambda \mu(\lambda) f(\lambda), \tag{157}$$

where:

$$\mu(\lambda) := \frac{\sqrt{4\sigma^2 - \lambda^2}}{2\pi\sigma^2}. \tag{158}$$

The Langevin equation can be rewritten in the eigenspace as:

$$\dot{T}_{\Lambda}(t) = -\frac{\partial \mathcal{H}}{\partial T_{\Lambda}} - \left(\sum_{c=1}^d \lambda_c \right) T_{\Lambda}(t) + \eta_{\Lambda}(t), \tag{159}$$

where $\Lambda := \{\lambda_1, \dots, \lambda_d\}$ and:

$$T_{\Lambda} := \sum_I T_{i_1 \dots i_d} \prod_{c=1}^d u_{i_c}^{(\lambda_c)}. \tag{160}$$

In the quenched regime for Φ_c , the solution for $T_{\Lambda}(t)$ reads:

$$T_{\Lambda}(t) = T_{\Lambda}(0)\rho(\Lambda, t) + \int_0^t dt' \eta_{\Lambda}(t') \frac{\rho(\Lambda, t)}{\rho(\Lambda, t')}, \tag{161}$$

where:

$$\rho(\Lambda, t) = e^{-g(t) - (\sum_{c=1}^d \lambda_c)t}. \tag{162}$$

Because the spectrum is bounded, i.e. $\int d\lambda \rho(\lambda) = 1$, no UV divergence is expected. Furthermore, because the eigenvectors $u_i^{(\lambda)}$ inherit the randomness of matrices σ_c , the condition:

$$T_{\Lambda}(0) = 1, \tag{163}$$

corresponds to a randomly distributed tensor $T_I(0)$ [6,5]. A closed equation can be deduced from the asymptotic condition:

$$U'(\kappa(t)) \rightarrow d \times 2\sigma, \tag{164}$$

and for this section we define $U(\kappa)$ as:

$$U(\kappa) = (\mu + d \times 2\sigma)\kappa + d \sum_{p \geq 2} \frac{g_p}{p} \kappa^p, \tag{165}$$

such that $\mu = 0$ remains the critical value. Despite these changes, equations remain essentially the same. For the quartic model, for instance, the closed equation reads again:

$$G(t) = -\frac{\bar{g}_2 d}{\mu} \left(H(t) + T F(t) \right), \tag{166}$$

where $G(t) := e^{2g(t)}$, $H(t)$ is now defined as:

$$H(t) := \int_{[-2\sigma, 2\sigma]^d} \left(\prod_{c=1}^d \mu(\lambda_c) d\lambda_c \right) e^{-2(\sum_{c=1}^d \lambda_c)t - 4d\sigma}, \tag{167}$$

and $F(t)$ is still defined as

$$F(t) := \int_0^t dt' H(t - t')G(t'). \tag{168}$$

The closed equation is solved as well using Laplace transform and is defined for $T < T_c$, with:

$$T_c = -\frac{\mu}{\bar{g}_2 d} \frac{1}{\bar{H}(0)} \equiv -\frac{\mu}{\bar{g}_2 d} (2\sigma)^d. \tag{169}$$

For higher order potential furthermore, the previous construction generalizes obviously, and we get $T_c^{(\mu)} = (2\sigma)^d \gamma_{\mu}$ in replacement of equation (133). As stressed above, the spectrum being bounded, no UV divergence is expected, despite the system exhibiting a non-trivial behavior for a large time. In particular, we recover that the memory of the initial condition does not vanish exponentially, and we have for the 2-point correlation function:

$$C(t) \sim \frac{1}{t^{3d/4}}, \tag{170}$$

and $U'(\kappa(t)) \rightarrow d \times 2\sigma + \mathcal{O}(t^{-1})$ for t large enough.

6. Discussions and conclusion

In this paper, we investigated the large-time behavior of a stochastic complex tensor in the cyclic melonic regime. We focused on the melonic kinetics and low-temperature regimes for different cases, including blank noise limit with Laplacian or tensorial disorder, and memory effects with temporal colored noise. One of the main particularities of the melonic kinetics, which occurs for rank $d > 3$ regarding kinetics for matrix or vector fields comes essentially from the ability of tensor to self-average without breaking symmetry at leading order (i.e. at the melonic order). Indeed, for vector fields, the kinetics describe a dynamical ordering resulting from the symmetry breaking for $U(N)$ or $O(N)$ symmetry. In the melonic case, the vacuum $(\Phi_c)_{ij} = \kappa \delta_{ij}$ commutes with any generator of the Lie algebra associated with this symmetry, which remains unbroken. In the case of the matrix fields, such a tractable vacuum for equilibrium dynamics is unexpected, because of the measured effect in the matrix path integral for equilibrium states, that repelled eigenvalues and leads to a non-trivial spectrum in the large N limit [11]. In contrast for the tensors fields, the measured effect is next to the leading order, and the eigenvalues for the intermediate fields collapse [12]. In this paper, we investigated some new aspects of the low-temperature behavior of the melonic kinetics, which is in connection with our recent contribution in the group field theory context [18]. Some aspects could be addressed in the future, including next to finite N effects and we may implement methods like renormalization group (see [27], in preparation). Furthermore, rigorous bounds for critical temperatures should be proved, rather than estimates provided in this work.

CRedit authorship contribution statement

All authors have contributed equally to all stages of the manuscript's completion.

Declaration of competing interest

The authors declare that they have no known competing financial interests or personal relationships that could have appeared to influence the work reported in this paper.

Data availability

No data was used for the research described in the article.

References

- [1] R. Livi, P. Politi, *Nonequilibrium Statistical Physics*, Cambridge University Press, 2017.
- [2] A.J. Bray, *Theory of phase-ordering kinetics*, *Adv. Phys.* 43 (3) (1994).
- [3] V. Lahoche, D. Ousmane Samary, *Low temperature dynamics for confined $p = 2$ soft spin in the quenched regime*, arXiv:2211.07809 [hep-th].
- [4] C.L. Emmott, A.J. Bray, *Phase-ordering dynamics with an order-parameter-dependent mobility: the large-n limit*, *Phys. Rev. E* 59 (1999) 213, Published 1 January.
- [5] I.G. Cirano De Dominicis, *Random Fields and Spin Glasses: A Field Theory Approach*, Cambridge University Press, 2009.
- [6] L.F. Cugliandolo, David S. Dean, *Full dynamical solution for a spherical spin-glass model*, *J. Phys. A* 28 (1995) 4213.
- [7] J. Kurchan, L.F. Cugliandolo, *Analytical solution of the off-equilibrium dynamics of a long range spin-glass model*, *Phys. Rev. Lett.* (1993).

- [8] Y.V. Fyodorov, A. Perret, G. Schehr, Large time zero temperature dynamics of the spherical $p=2$ -spin glass model of finite size, *J. Stat. Mech. Theory Exp.* 2015 (11) (2015) P11017.
- [9] V. Lahoche, D. Ousmane Samary, Low temperature expansion for $p=2$ -soft spin dynamics, arXiv:2211.07809, 2022.
- [10] V. Lahoche, D. Ousmane Samary, M. Tamaazousti, Functional renormalization group for multilinear disordered Langevin dynamics II: revisiting the $p=2$ spin dynamics for Wigner and Wishart ensembles, arXiv:2212.05649 [hep-th].
- [11] P. Francesco, P. Ginsparg, J. Zinn-Justin, 2D gravity and random matrices, *Phys. Rep.* 254 (1–2) (1995) 1–133.
- [12] R. Gurau, *Random Tensors*, Oxford University Press, 2017.
- [13] V. Bonzom, R. Gurau, V. Rivasseau, Random tensor models in the large N limit: uncoloring the colored tensor models, *Phys. Rev. D* 85 (8) (2012) 084037.
- [14] G. Eyal, M. Moshe, S. Nishigaki, J. Zinn-Justin, The $O(N)$ vector model in the large- N limit revisited: multicritical points and double scaling limit, *Nucl. Phys. B* 470 (3) (1996) 369–395.
- [15] V. Bonzom, R. Gurau, A. Riello, V. Rivasseau, Critical behavior of colored tensor models in the large N limit, *Nucl. Phys. B* 853 (2011) 174–195.
- [16] D. Oriti, Disappearance and emergence of space and time in quantum gravity, *Stud. Hist. Philos. Sci. B Stud. Hist. Philos. Modern Phys.* 46 (2014) 186–199.
- [17] V. Bonzom, R. Gurau, J.P. Ryan, A. Tanasa, The double scaling limit of random tensor models, *J. High Energy Phys.* 2014 (2014) 051.
- [18] V. Lahoche, D. Ousmane Samary, Stochastic dynamics for group field theories, arXiv preprint, arXiv:2209.02321, 2023.
- [19] R.A. Handelsman, J.S. Lew, Asymptotic expansion of Laplace transforms near the origin, *SIAM J. Math. Anal.* 1 (1) (1970).
- [20] J. Zinn-Justin, *From Random Walks to Random Matrices*, Oxford Graduate Texts, 2019.
- [21] M. Chupeau, J. Gladrow, A. Chepelianski, U.F. Keyser, E. Trizac, Optimizing Brownian escape rates by potential shaping, *Proc. Natl. Acad. Sci.* 117 (3) (2020) 1383–1388.
- [22] P.B. Burada, B. Lindner, Escape rate of an active Brownian particle over a potential barrier, *Phys. Rev. E* 85 (3) (2012) 032102.
- [23] P.B. Visscher, Escape rate for a Brownian particle in a potential well, *Phys. Rev. B* 13 (8) (1976) 3272.
- [24] A. Berera, J. Mabillard, B.W. Mintz, R.O. Ramos, Formulating the Kramers problem in field theory, *Phys. Rev. D* 100 (7) (2019) 076005.
- [25] V.I. Melnikov, The Kramers problem: fifty years of development, *Phys. Rep.* 209 (1–2) (1991) 1–71.
- [26] A. Kamenev, *Field Theory of Non-equilibrium Systems*, Cambridge University Press, 2023.
- [27] H. Erbin, V. Lahoche, D. Ousmane Samary, S.F. Zime Yerima, Finite N effects and large N limit for stochastic tensor fields renormalization group, In preparation (expected 2023).
- [28] R. Gurau, The complete $1/N$ expansion of a SYK-like tensor model, *Nucl. Phys. B* 916 (2017) 386–401, <https://doi.org/10.1016/j.nuclphysb.2017.01.015>, arXiv:1611.04032 [hep-th].
- [29] I.R. Klebanov, G. Tarnopolsky, Uncolored random tensors, melon diagrams, and the Sachdev-Ye-Kitaev models, *Phys. Rev. D* 95 (4) (2017) 046004, <https://doi.org/10.1103/PhysRevD.95.046004>, arXiv:1611.08915 [hep-th].
- [30] J. Maldacena, D. Stanford, Remarks on the Sachdev-Ye-Kitaev model, *Phys. Rev. D* 94 (10) (2016) 106002, <https://doi.org/10.1103/PhysRevD.94.106002>, arXiv:1604.07818 [hep-th].
- [31] S. Choudhury, K. Shirish, Wormhole calculus without averaging from $O(N)^{q-1}$ tensor model, *Phys. Rev. D* 105 (4) (2022) 046002, <https://doi.org/10.1103/PhysRevD.105.046002>, arXiv:2106.14886 [hep-th].
- [32] S. Choudhury, A. Dey, I. Halder, L. Janagal, S. Minwalla, R. Poojary, Notes on melonic $O(N)^{q-1}$ tensor models, *J. High Energy Phys.* 06 (2018) 094, [https://doi.org/10.1007/JHEP06\(2018\)094](https://doi.org/10.1007/JHEP06(2018)094), arXiv:1707.09352 [hep-th].
- [33] V. Bonzom, T. Delpeuvre, V. Rivasseau, Enhancing non-melonic triangulations: a tensor model mixing melonic and planar maps, *Nucl. Phys. B* 895 (2015) 161–191, <https://doi.org/10.1016/j.nuclphysb.2015.04.004>, arXiv:1502.01365 [math-ph].
- [34] C.M. Chang, S. Colin-Ellerin, M. Rangamani, On melonic supertensor models, *J. High Energy Phys.* 10 (2018) 157, [https://doi.org/10.1007/JHEP10\(2018\)157](https://doi.org/10.1007/JHEP10(2018)157), arXiv:1806.09903 [hep-th].
- [35] I.R. Klebanov, G. Tarnopolsky, On large N limit of symmetric traceless tensor models, *J. High Energy Phys.* 10 (2017) 037, [https://doi.org/10.1007/JHEP10\(2017\)037](https://doi.org/10.1007/JHEP10(2017)037), arXiv:1706.00839 [hep-th].
- [36] K. Bulycheva, I.R. Klebanov, A. Milekhin, G. Tarnopolsky, Spectra of operators in large N tensor models, *Phys. Rev. D* 97 (2) (2018) 026016, <https://doi.org/10.1103/PhysRevD.97.026016>, arXiv:1707.09347 [hep-th].
- [37] I.R. Klebanov, P.N. Pallegar, F.K. Popov, Majorana fermion quantum mechanics for higher rank tensors, *Phys. Rev. D* 100 (8) (2019) 086003, <https://doi.org/10.1103/PhysRevD.100.086003>, arXiv:1905.06264 [hep-th].